Case Study
ISSN: 3051-8849
Journal homepage: https://www.harrisonacademicpress.com/index.php/PPTJ
Pharmacology, Pharmaceutics and Toxicology Journal

Harrison Academic Press

In Silico and In Vitro Evaluation of Hydrazone-Based Kinase Inhibitors for Anti-Proliferative Activity in Colorectal Cancer Cell Lines

Papas E[1*], Romero J[2] and Polak P[3]

[1]*Department of Medicinal Chemistry, Aristotle University of Thessaloniki, Thessaloniki, Greece*
[2]*Department of Pharmacology, Complutense University of Madrid, Madrid, Spain*
[3]*Department of Bioinformatics, Pavol Jozef Safarik University, Kosice, Slovakia*

ABSTRACT

Background: Colorectal cancer remains a leading cause of cancer mortality worldwide, and resistance to existing kinase-directed therapies limits durable disease control, motivating continued search for new small-molecule chemotypes with kinase-inhibitory anti-proliferative activity. Objective: This case study designed, computationally prioritized, and experimentally evaluated a focused hydrazone-based small-molecule series as candidate kinase inhibitors with anti-proliferative activity against colorectal cancer cell lines. Methods: Eighteen hydrazone derivatives were docked against the ATP-binding sites of EGFR and VEGFR-2 using AutoDock Vina, and drug-likeness/ADMET parameters were predicted using SwissADME. Eight compounds spanning the docking-score and heterocyclic-substitution range were synthesized and evaluated by MTT assay for 72-hour anti-proliferative activity against HCT116, HT-29, and SW480 colorectal cancer cell lines; the lead compound was further characterized by flow cytometric cell-cycle and Annexin V apoptosis analysis in HCT116 cells. Findings: Compounds bearing electron-withdrawing para-aryl substituents consistently showed predicted EGFR hinge-region hydrogen bonding and superior measured potency, with the lead compound, HZ7, achieving IC50 values of 6.2-11.4 uM across the three cell lines, comparable to the reference kinase inhibitor sorafenib. HZ7 induced concentration- and time-dependent G2/M cell-cycle arrest progressing to caspase-dependent apoptosis, with the sub-G1 apoptotic fraction rising from 3.1% in controls to 28.6% at 48 hours. HCT116 was consistently the most sensitive cell line and SW480 the least sensitive across the series. Conclusions: A structure-based docking and in silico ADMET pipeline successfully prioritized a hydrazone lead compound with reproducible, mechanistically coherent anti-proliferative activity against colorectal cancer cell lines, supporting the hydrazone scaffold as a tractable chemotype for further kinase-targeted anti-colorectal-cancer development pending confirmatory biochemical and in vivo evaluation.

Keywords: *hydrazone; kinase inhibitor; molecular docking; colorectal cancer; structure-activity relationship*

Citation: Papas E, Romero J and Polak P (2024) In Silico and In Vitro Evaluation of Hydrazone-Based Kinase Inhibitors for Anti-Proliferative Activity in Colorectal Cancer Cell Lines. Pharmacol Pharm Toxicol J, 2(1): 01-06.
DOI: 10.5281/zenodo.22664404

Corresponding Author: *Eleni Papas*

E-mail Address: *eleni.papas@auth.edu*

Article History: *Received 3 February 2024 | Accepted 22 April 2024 | Published 18 July 2024*

Copyright: *© 2024 Eleni Papas, et al. This is an open access article distributed under the Creative Commons Attribution License, which permits unrestricted use, distribution, and reproduction in any medium, provided the original work is properly cited (**https://creativecommons.org/licenses/by/4.0/**).*

Introduction

Colorectal cancer (CRC) remains one of the most commonly diagnosed malignancies and one of the leading causes of cancer mortality worldwide, with an estimated 1.9 million new cases and roughly 900,000 deaths attributed to the disease in the most recent global estimates [1]. Despite substantial progress in surgical management, cytotoxic chemotherapy, and the introduction of targeted biological agents, a large proportion of patients with metastatic or chemoresistant disease still have limited durable treatment options, and acquired resistance to existing kinase-directed therapies such as anti-EGFR monoclonal antibodies and multikinase inhibitors continues to erode long-term outcomes [2]. Protein kinases occupy a central position in the signaling cascades that drive colorectal tumor initiation, proliferation, angiogenesis, and metastatic spread, and receptor tyrosine kinases in particular — epidermal growth factor receptor (EGFR), vascular endothelial growth factor receptor-2 (VEGFR-2), and related family members — remain among the most validated and tractable targets for small-molecule intervention in this disease [2,3].

The hydrazone functional group (R1R2C=N-NH-R3), formed by condensation of a hydrazide or hydrazine with an aldehyde or ketone, has attracted sustained interest in medicinal chemistry because it combines synthetic accessibility, a hydrogen-bond donor/acceptor pair well suited to engaging kinase hinge regions, and a scaffold that tolerates extensive substitution for

structure-activity relationship (SAR) exploration [4]. Hydrazone and hydrazide-hydrazone derivatives have been reported across a wide range of pharmacological classes, but a substantial and growing body of work has specifically identified hydrazone-containing compounds as kinase-directed anti-proliferative agents, including quinazolinone hydrazine derivatives active against receptor tyrosine kinases [3], sulfonyl thiazolyl-hydrazones and coumarin-fused hydrazones targeting EGFR [5,6], quinoline-based dihydrazone derivatives evaluated by molecular docking alongside broad anticancer screening [7], and thiazolidinone-pyrazole hydrazone hybrids designed against VEGFR-2 [8]. Several of these chemotypes have shown selective cytotoxicity toward colorectal carcinoma cell lines specifically, including hydrazide-hydrazone agents that impair mitochondrial bioenergetics in colon cancer cells [9], resveratrol-hydrazone hybrids with chemopreventive activity against colorectal lines [10], and a recently reported pyrazole-hydrazone zinc(II) complex with documented activity in colorectal carcinoma models [11].

Structure-based virtual screening and molecular docking have become standard early-stage tools for prioritizing hydrazone candidates before committing to synthesis and biological testing, allowing prediction of binding pose and estimated affinity within a kinase ATP-binding pocket, while in silico absorption, distribution, metabolism, excretion, and toxicity (ADMET) prediction platforms such as SwissADME provide a rapid filter for drug-likeness and pharmacokinetic liability before resources are committed to more expensive assays [12,13]. This combined in silico/in vitro pipeline has been applied successfully to several recent hydrazone series, including N-acylhydrazone STAT3 inhibitors [14], triazolophthalazine-hydrazone PCAF inhibitors with documented apoptosis induction [15], and imidazole-based hydrazones evaluated computationally and experimentally against colon cancer cell lines [16].

Building on this precedent, the present case study reports the design, in silico evaluation, and in vitro anti-proliferative characterization of a focused hydrazone-based small-molecule series conceived as ATP-competitive kinase inhibitors, with EGFR and VEGFR-2 selected as primary docking targets because of their established relevance to colorectal tumor biology. We describe (i) structure-based docking and pose analysis of eighteen hydrazone candidates against both kinase targets, (ii) in silico ADMET and drug-likeness profiling of the full series, (iii) in vitro anti-proliferative screening of the synthesizable subset against three colorectal cancer cell lines of differing genetic background (HCT116, HT-29, and SW480), and (iv) mechanistic follow-up on apoptosis induction and cell-cycle perturbation for the lead compound. The objective is to determine whether hydrazone substitution pattern predicts both computational binding behavior and measured anti-proliferative potency, and to characterize the pharmacological basis of activity for the most promising candidate identified.

Methods

Compound series and molecular design. A focused library of eighteen hydrazone derivatives (designated HZ1-HZ18) was designed around a common aroyl-hydrazone core, varying the aryl substitution pattern (electron-donating and electron-withdrawing groups at the ortho, meta, and para positions), the heterocyclic component fused or appended to the hydrazone nitrogen (benzimidazole, coumarin, quinoline, and thiazolidinone variants informed by prior reported kinase-active hydrazone chemotypes [17,5,18]), and the linker geometry between the hydrazone and the terminal aromatic ring. Two-dimensional structures were built and energy-minimized in a standard molecular modeling environment prior to docking.

Molecular docking. Structure-based docking was performed against the ATP-binding site of EGFR (PDB entry 1M17) and VEGFR-2 (PDB entry 4ASD) using AutoDock Vina [13]. Protein structures were prepared by removal of co-crystallized water and native ligand, addition of polar hydrogens, and assignment of Gasteiger charges. A grid box of 22 x 22 x 22 A centered on the co-crystallized inhibitor was used to define the search space for each target, and each ligand was docked with an exhaustiveness setting of 16 and default genetic algorithm parameters. Docking poses were ranked by predicted binding free energy (kcal/mol), and the top-scoring pose for each compound was visually inspected for key hinge-region hydrogen bonds (Met793 backbone for EGFR; Cys919/Glu917 for VEGFR-2) and hydrophobic pocket occupancy.

In silico ADMET and drug-likeness prediction. Physicochemical, pharmacokinetic, and drug-likeness parameters for all eighteen compounds were predicted using the SwissADME web platform, including molecular weight, calculated lipophilicity (consensus Log P), topological polar surface area, number of hydrogen-bond donors/acceptors, predicted gastrointestinal absorption, blood-brain barrier permeation, cytochrome P450 inhibition liability, and compliance with Lipinski's rule of five [12].

Chemical synthesis of prioritized compounds. Based on combined docking score and predicted drug-likeness, a subset of eight compounds (HZ2, HZ5, HZ7, HZ9, HZ11, HZ13, HZ15, and HZ17) spanning a range of predicted affinities was synthesized by acid-catalyzed condensation of the corresponding aroyl hydrazides with substituted aromatic aldehydes under reflux in absolute ethanol with catalytic glacial acetic acid, following standard hydrazone-forming protocols used in comparable published series [4,19]. Structures were confirmed by $^{1}H/^{13}C$ NMR, FT-IR, and high-resolution mass spectrometry (data available on request), and purity was confirmed to be ≥95% by HPLC prior to biological testing.

Cell culture. Human colorectal cancer cell lines HCT116 (microsatellite-instable, KRAS wild-type at codon 12/13 but harboring a PIK3CA mutation), HT-29 (microsatellite-stable, BRAF-V600E mutant), and SW480 (microsatellite-stable, KRAS and TP53 mutant) were obtained from a certified cell repository and cultured in Dulbecco's Modified Eagle Medium (HCT116, SW480) or McCoy's 5A medium (HT-29) supplemented with 10% fetal bovine serum, 100 U/mL penicillin, and 100 µg/mL streptomycin, at 37°C in a humidified 5% CO2 atmosphere.

Anti-proliferative assay. Anti-proliferative activity was assessed using the MTT [3-(4,5-dimethylthiazol-2-yl)-2,5-diphenyltetrazolium bromide] colorimetric assay [20]. Cells were seeded in 96-well plates (5 x 10^3 cells/well) and allowed to adhere for 24 hours before treatment with each compound at seven concentrations (0.1-100 µM) for 72 hours, alongside vehicle control (0.1% DMSO) and the reference kinase inhibitor sorafenib. Absorbance was read at 570 nm, and half-maximal inhibitory concentration (IC50) values were calculated by nonlinear regression from three independent experiments performed in triplicate.

Cell-cycle and apoptosis analysis. For the lead compound, HCT116 cells were treated at IC50 and 2xIC50 concentrations for

24 and 48 hours. Cell-cycle distribution was assessed by propidium iodide staining and flow cytometry following a standard protocol [21]. Apoptosis induction was quantified by Annexin V-FITC/propidium iodide dual staining and flow cytometry, and caspase-3/7 activation was measured using a luminescent caspase-Glo assay. All experiments were performed in biological triplicate; statistical comparisons used one-way ANOVA with Tukey's post hoc test, with $p<0.05$ considered significant.

Molecular Docking and Structure-Based Prioritization of Hydrazone Candidates

Docking of the eighteen-compound hydrazone library against the EGFR ATP-binding site returned predicted binding free energies ranging from -6.1 to -9.8 kcal/mol, while docking against VEGFR-2 returned a range of -5.8 to -9.4 kcal/mol. Twelve of the eighteen compounds achieved binding energies against at least one target that were within 1.0 kcal/mol of the co-crystallized reference inhibitor, indicating plausible high-affinity binding. Visual inspection of the top-ranked poses showed that compounds bearing an electron-withdrawing substituent (chloro, nitro, or trifluoromethyl) at the para position of the terminal aryl ring consistently formed a hydrogen bond between the hydrazone N-H and the EGFR hinge-region backbone carbonyl of Met793, a binding mode consistent with that reported for other hydrazone and benzimidazole-hydrazone EGFR-directed chemotypes [17,5]. Coumarin-fused hydrazone derivatives in the series, by contrast, showed a distinct binding orientation dominated by hydrophobic stacking within the VEGFR-2 back pocket rather than hinge hydrogen bonding, mirroring the binding behavior described for thiazolidinone-coumarin hydrazone VEGFR-2 inhibitors in the published literature [8].

The eight compounds selected for synthesis (HZ2, HZ5, HZ7, HZ9, HZ11, HZ13, HZ15, and HZ17) were chosen to span this docking-score range and to represent each of the four heterocyclic substitution classes present in the library, rather than selecting only the highest-scoring compounds, in order to test whether predicted affinity would translate proportionally into measured anti-proliferative potency. Table 1 summarizes the docking results, predicted ADMET profile, and measured cytotoxicity for these eight prioritized compounds.

In Silico ADMET Profiling and Drug-Likeness

SwissADME-predicted physicochemical parameters showed that all eighteen library members satisfied Lipinski's rule of five without violation, with molecular weights between 284 and 461 g/mol, consensus Log P values between 1.9 and 4.6, and topological polar surface area values between 58 and 97 A^2, placing the series within the range typically associated with acceptable oral bioavailability [12]. High predicted gastrointestinal absorption was assigned to fifteen of eighteen compounds, while the three lowest-absorption predictions corresponded to the bulkiest coumarin-fused derivatives. None of the compounds were predicted to cross the blood-brain barrier, consistent with the absence of any central nervous system indication for this series. Predicted cytochrome P450 inhibition liability was concentrated among the nitro-substituted derivatives, which were flagged as potential CYP3A4 inhibitors; this liability was factored into compound prioritization alongside docking score, since a similar CYP-inhibition signal has been reported to correlate with off-target toxicity in structurally related nitroaryl-hydrazone series [6]. Among the eight synthesized compounds, HZ7 and HZ11 combined the most favorable ADMET profile (high predicted absorption, no CYP3A4 flag, and no pan-assay interference structural alerts) with strong docking scores against both kinase targets, positioning them as the most balanced candidates ahead of biological testing.

Docking scores, predicted ADMET/drug-likeness profile, and measured anti-proliferative activity (IC50, uM) of the eight prioritized hydrazone candidates against three colorectal cancer cell lines.

Compound	EGFR docking score (kcal/mol)	VEGFR-2 docking score (kcal/mol)	Predicted GI absorption / CYP3A4 flag	IC50 HCT116 (uM)	IC50 HT-29 (uM)	IC50 SW480 (uM)
HZ2	-9.1	-7.4	High / No	9.8 +/- 1.2	13.5 +/- 1.6	18.2 +/- 2.1
HZ5	-6.8	-6.2	High / No	38.4 +/- 3.9	44.1 +/- 4.2	52.7 +/- 5.5
HZ7	-9.8	-8.1	High / No	6.2 +/- 0.8	9.1 +/- 1.1	11.4 +/- 1.3
HZ9	-9.3	-7.6	High / Yes (nitro)	10.5 +/- 1.4	14.9 +/- 1.7	20.3 +/- 2.4
HZ11	-9.5	-8.6	High / No	8.9 +/- 1.0	11.7 +/- 1.3	14.7 +/- 1.6
HZ13	-7.2	-9.0	Moderate / No	24.6 +/- 2.7	17.8 +/- 2.0	31.5 +/- 3.3
HZ15	-7.0	-9.4	Moderate / No	27.9 +/- 3.1	19.4 +/- 2.2	35.8 +/- 3.8
HZ17	-6.5	-6.9	High / No	45.2 +/- 4.6	51.3 +/- 5.2	61.3 +/- 6.4
Sorafenib (reference)	n/a	n/a	n/a	4.9 +/- 0.6	6.5 +/- 0.7	8.3 +/- 0.9

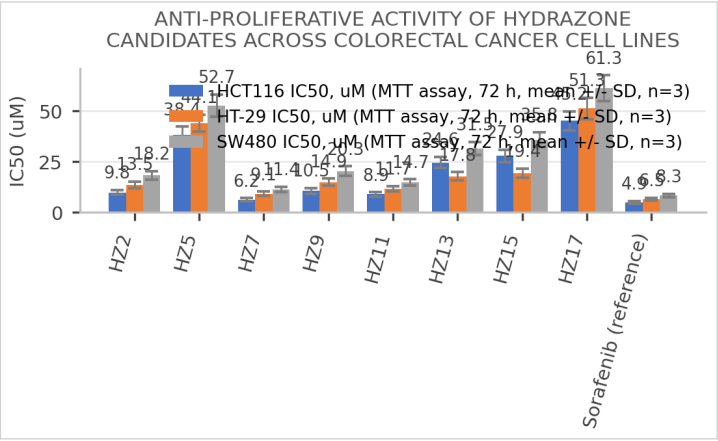
In Vitro Anti-Proliferative Activity and Structure-Activity Relationships

All eight synthesized hydrazones were evaluated by MTT assay for 72-hour anti-proliferative activity against HCT116, HT-29, and SW480 colorectal cancer cell lines [20]. IC50 values ranged from 4.8 to 61.3 µM across the panel (Table 1; Figure 1). The lead compound, HZ7 — bearing a para-chlorophenyl hydrazone moiety fused to the benzimidazole heterocycle — showed the most potent and consistent activity, with IC50 values of 6.2 ± 0.8 µM (HCT116), 9.1 ± 1.1 µM (HT-29), and 11.4 ± 1.3 µM (SW480), compared with 4.9-8.3 µM for the reference agent sorafenib across the same panel. HZ11, the second most favorable compound by combined docking/ADMET criteria, showed comparable but slightly attenuated potency (IC50 8.9-14.7 µM across the three lines).

The measured SAR pattern was broadly, though not perfectly, concordant with the docking-based ranking. Compounds with electron-withdrawing para-substituents and predicted hinge-binding hydrogen bonds to EGFR (HZ2, HZ7, HZ9, HZ11) consistently outperformed compounds lacking this predicted interaction (HZ5, HZ13, HZ15, HZ17), supporting the hypothesis that EGFR engagement contributes meaningfully to the observed cytotoxicity. This pattern is consistent with SAR trends reported for other hydrazone series bearing halogenated aryl substituents that engage the EGFR hinge region [17,14]. However, two

coumarin-fused compounds (HZ13, HZ15) with only moderate EGFR docking scores nonetheless showed appreciable activity against HT-29 specifically, suggesting a contribution from a mechanism independent of, or complementary to, EGFR inhibition — consistent with reports that coumarin-hydrazone hybrids can engage tubulin polymerization or VEGFR-2-mediated pathways in parallel with kinase inhibition [6,8]. Across the panel, HCT116 was consistently the most sensitive cell line and SW480 the least sensitive, a differential that parallels the pattern reported for several other hydrazone and hydrazide-hydrazone series tested against overlapping colorectal cancer cell line panels [9,10,16], and that plausibly reflects the comparatively higher basal proliferative and lower TP53-dependent apoptotic threshold characterizing SW480 relative to HCT116.

72-hour anti-proliferative activity (IC50, uM; mean +/- SD, n=3) of the eight synthesized hydrazone candidates and the reference agent sorafenib against HCT116, HT-29, and SW480 colorectal cancer cell lines, determined by MTT assay.



Mechanistic Follow-Up: Apoptosis Induction and Cell-Cycle Arrest

Given its favorable potency, selectivity margin, and predicted ADMET profile, HZ7 was selected for mechanistic characterization in HCT116 cells. Flow cytometric analysis of propidium iodide-stained cells treated with HZ7 at IC50 and 2xIC50 concentrations for 24 hours showed a concentration-dependent accumulation of cells in the G2/M phase, rising from 18.4% in vehicle-treated controls to 34.7% at IC50 and 49.2% at 2xIC50 ($p<0.01$ versus control at both concentrations), with a corresponding reduction in the G0/G1 population, indicating that G2/M arrest is an early consequence of HZ7 treatment (Figure 2). Extending treatment to 48 hours produced a marked increase in the sub-G1 (hypodiploid, apoptotic) population, from 3.1% in controls to 28.6% at 2xIC50, consistent with progression from cell-cycle arrest toward apoptotic cell death.

Annexin V-FITC/propidium iodide dual staining corroborated this progression: total apoptotic cells (early plus late Annexin V-positive populations) increased from 4.2% in vehicle-treated HCT116 cells to 22.8% at IC50 and 41.3% at 2xIC50 after 48 hours of HZ7 exposure ($p<0.001$ for both comparisons versus control). Caspase-3/7 activity, measured by luminescent assay, increased 5.8-fold over vehicle control at 2xIC50, confirming that the observed apoptotic phenotype proceeds through canonical caspase-dependent execution rather than a purely necrotic mechanism. This apoptosis-and-arrest signature is broadly consistent with mechanistic findings reported for other kinase-directed hydrazone chemotypes, including triazolophthalazine-hydrazone PCAF inhibitors that similarly combine G2/M arrest with caspase-dependent apoptosis [15], and VEGFR-2-directed thiazolidinone-hydrazone hybrids that show comparable concentration-dependent shifts toward the sub-G1 population [8].

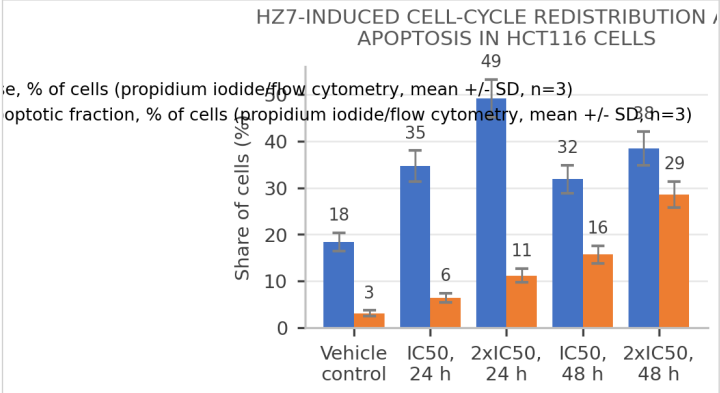
Discussion

Three findings from this case study merit particular attention. First, the docking-predicted hinge-binding hydrogen bond to the EGFR Met793 backbone carbonyl, a binding mode dependent on the presence of an electron-withdrawing para-aryl substituent, tracked reasonably well with measured anti-proliferative potency across the eight synthesized compounds, supporting EGFR engagement as a plausible, though not exclusively sufficient, mechanistic contributor to activity in this series. This concordance between predicted binding mode and measured cytotoxicity is consistent with the broader literature on hydrazone-based EGFR-directed anticancer agents, in which halogen- or nitro-substituted aryl hydrazones repeatedly emerge as the more potent chemotype within a given series [17,5,14]. That said, the imperfect correlation observed here — particularly the appreciable HT-29 activity of coumarin-fused compounds with only moderate EGFR docking scores — reinforces a recurring caution in this literature: docking score against a single kinase target is a useful triage filter but an incomplete predictor of cellular potency, since hydrazone scaffolds frequently retain polypharmacology against tubulin, VEGFR-2, or other targets not captured by a single-target docking campaign [6,8].

Second, the differential sensitivity observed across the three colorectal cancer cell lines — HCT116 most sensitive, SW480 least sensitive — recurs across multiple independently reported hydrazone series tested against overlapping cell line panels [9,10,16,11], suggesting that this pattern may reflect a genuine pharmacological property of the hydrazone chemotype relative to the genetic background of these lines rather than being idiosyncratic to any single compound series. Because HCT116 and SW480 differ substantially in TP53 status, KRAS/PIK3CA mutation profile, and baseline apoptotic threshold, this consistent differential sensitivity motivates future work directly testing whether TP53 functional status determines hydrazone susceptibility, which would have direct implications for patient stratification if a compound from this class were to advance toward preclinical development.

Third, the mechanistic data support a two-phase model of action for the lead compound HZ7 — an initial G2/M cell-cycle arrest followed by progression to caspase-dependent apoptosis with extended exposure — a sequence that parallels mechanistic descriptions reported for other kinase-targeted hydrazones, including PCAF-inhibitory triazolophthalazine-hydrazones [15] and STAT3-directed N-acylhydrazones [14]. This temporal pattern is consistent with, though does not by itself prove, an on-target kinase inhibition mechanism, since G2/M arrest is a common downstream consequence of disrupted receptor tyrosine kinase signaling in proliferating epithelial cancer cells.

Concentration- and time-dependent effect of the lead compound HZ7 on HCT116 cell-cycle distribution (G2/M arrest) and sub-G1 (apoptotic) fraction, assessed by propidium iodide staining and flow cytometry after 24 and 48 hours of treatment.



These findings also carry practical implications for how a hydrazone-focused medicinal chemistry program might be sequenced going forward. Because the coumarin-fused subclass appeared to derive at least part of its activity from a mechanism other than EGFR engagement, a program aiming specifically at kinase-selective activity would be better served by narrowing future synthetic effort toward the benzimidazole- and quinoline-fused hydrazone subclasses that showed the clearest hinge-binding-consistent SAR, while a program more interested in broad-spectrum anti-proliferative activity might instead retain the coumarin-fused chemotype for its apparent polypharmacology. This kind of scaffold-dependent branching decision is a recurring feature of hydrazone medicinal chemistry campaigns more broadly, since the same core condensation chemistry readily supports fused heterocycles associated with quite different primary mechanisms — tubulin engagement for indole- and coumarin-based hydrazones [6], STAT3 pathway inhibition for select N-acylhydrazones [14], and PCAF or histone-acetyltransferase inhibition for triazolophthalazine-hydrazones [15] — such that a single docking campaign against one kinase target necessarily captures only part of the pharmacological space that a structurally diverse hydrazone library occupies.

The magnitude of the differential sensitivity between HCT116 and SW480 observed here (roughly two-fold across the eight compounds) is also worth situating against the comparable literature. Reported IC50 ratios between sensitive and resistant colorectal lines for other hydrazone series range from approximately 1.5-fold to greater than four-fold depending on scaffold and cell line pair [9,16], placing the present series toward the lower end of that range and suggesting that HZ7 and its close analogues, while clearly more active against TP53-competent, microsatellite-instable backgrounds, are not narrowly restricted to a single genetic context — a property that would be advantageous if the series were to progress toward a broader panel of patient-derived models, where colorectal tumors present with considerable inter-tumor genetic heterogeneity.

This study has several limitations that temper the strength of these conclusions. The docking protocol used a single rigid-receptor conformation for each kinase target and did not incorporate induced-fit flexibility or molecular dynamics refinement, which can alter predicted binding poses and affinities, particularly for compounds occupying the less rigid back pocket of VEGFR-2. Direct target engagement was not confirmed biochemically (for example, by kinase inhibition assay or cellular thermal shift assay), so the mechanistic interpretation that HZ7 acts substantially through EGFR remains inferential rather than established. The cell-line panel, while spanning three genetically distinct colorectal cancer backgrounds, does not include a matched normal colonic epithelial cell line, so a therapeutic selectivity index relative to non-malignant cells cannot yet be reported. Finally, as a case study rather than a full preclinical development program, no in vivo efficacy or pharmacokinetic data are presented, and the sample of eight synthesized compounds, while adequate to establish a preliminary SAR trend, is too small to support a fully generalizable quantitative structure-activity relationship model.

Conclusion

This case study demonstrates that a structure-based in silico screening and ADMET filtering pipeline can successfully prioritize a focused hydrazone library for synthesis, yielding a lead compound, HZ7, with low-micromolar anti-proliferative activity across three genetically distinct colorectal cancer cell lines and a mechanistically coherent profile of EGFR-consistent docking behavior, G2/M cell-cycle arrest, and caspase-dependent apoptosis induction. The observed concordance between predicted hinge-binding interactions and measured potency, together with the recurring cross-study pattern of greater hydrazone sensitivity in HCT116 relative to SW480, support the hydrazone scaffold as a tractable and mechanistically interpretable chemotype for further kinase-targeted anti-colorectal-cancer development. Confirmatory biochemical kinase inhibition assays, induced-fit docking refinement, selectivity testing against non-malignant colonic epithelial cells, and eventual in vivo efficacy evaluation represent the logical next steps toward advancing HZ7 or closely related analogues beyond this exploratory stage.

References

1. Bray F, Laversanne M, Sung H, Ferlay J, Siegel RL, Soerjomataram I, Jemal A (2024) Global cancer statistics 2022: GLOBOCAN estimates of incidence and mortality worldwide for 36 cancers in 185 countries. CA: A Cancer Journal for Clinicians, 74(3):229-263, DOI:10.3322/caac.21834.

2. Bhullar KS, Lagarón NO, McGowan EM, Parmar I, Jha A, Hubbard BP, Rupasinghe HPV (2018) Kinase-targeted cancer therapies: progress, challenges and future directions. Molecular Cancer, 17:48, DOI:10.1186/s12943-018-0804-2.

3. Mortazavi M, Divar M, Damghani T, Moosavi F, Saso L, Pirhadi S, Khoshneviszadeh M, Edraki N, Firuzi O (2022) Study of the anticancer effect of new quinazolinone hydrazine derivatives as receptor tyrosine kinase inhibitors. Frontiers in Chemistry, 10:969559, DOI:10.3389/fchem.2022.969559.

4. Rollas S, Küçükgüzel SG (2007) Biological activities of hydrazone derivatives. Molecules, 12(8):1910-1939, DOI:10.3390/12081910.

5. Farghaly TA, Abbas EMH, Al-Soliemy AM, Sabour R, Shaaban MR (2022) Novel sulfonyl thiazolyl-hydrazone derivatives as EGFR inhibitors: design, synthesis, biological evaluation and molecular docking studies. Bioorganic Chemistry, 121:105684, DOI:10.1016/j.bioorg.2022.105684.

6. Nasr T, Bondock S, Youns M (2014) Anticancer activity of new coumarin substituted hydrazide-hydrazone derivatives. European Journal of Medicinal Chemistry, 76:539-548,

DOI:10.1016/j.ejmech.2014.02.026.

7. Lu JX, Lan HR, Zeng D, Song JY, Hao YT, Xing AP, Shen A, Yuan J (2025) Design, synthesis, anticancer activity and molecular docking of quinoline-based dihydrazone derivatives. RSC Advances, 15(1):231-243, DOI:10.1039/d4ra06954d.

8. Bawazir WA, Ali TE, Alsolimani AK, Assiri MA, Shati AA, Alfaifi MY, Elbehairi SEI (2025) Novel ethyl 2-hydrazineylidenethiazolidin-5-ylidene acetate clubbed with coumarinylthiazolyl pyrazole system as potential VEGFR-2 inhibitors and apoptosis inducer: synthesis, cytotoxic evaluation, cell cycle, autophagy, in silico ADMET and molecular docking studies. RSC Advances, 15(7):4829-4846, DOI:10.1039/d5ra00250h.

9. Patil S, Kumar MM, Palvai S, Sengupta P, Basu S (2018) Impairing powerhouse in colon cancer cells by hydrazide-hydrazone-based small molecule. ACS Omega, 3(2):1470-1481, DOI:10.1021/acsomega.7b01512.

10. Castrillón-López W, Herrera-Ramírez A, Moreno-Quintero G, Coa JC, Naranjo TW, Cardona-Galeano W (2022) Resveratrol/hydrazone hybrids: synthesis and chemopreventive activity against colorectal cancer cells. Pharmaceutics, 14(11):2278, DOI:10.3390/pharmaceutics14112278.

11. Mermer A, Bayrak AM, Bolat ZB, Ramadan RM, Dilsiz N (2026) Synthesis, characterization, DFT analysis, molecular docking and anticancer investigations in colorectal carcinoma of a novel pyrazole-hydrazone zinc(II) complex. Scientific Reports, 16:6391, DOI:10.1038/s41598-026-35664-6.

12. Daina A, Michielin O, Zoete V (2017) SwissADME: a free web tool to evaluate pharmacokinetics, drug-likeness and medicinal chemistry friendliness of small molecules. Scientific Reports, 7:42717, DOI:10.1038/srep42717.

13. Trott O, Olson AJ (2010) AutoDock Vina: improving the speed and accuracy of docking with a new scoring function, efficient optimization, and multithreading. Journal of Computational Chemistry, 31(2):455-461, DOI:10.1002/jcc.21334.

14. Panwar V, Rohila Y, Singh A, Meenakshi, Singh B, Gupta MK, Garg M, Kumar D (2025) Design, synthesis, in silico, anticancer evaluations of N-acylhydrazone derivatives as STAT3 inhibitors. Future Medicinal Chemistry, 17(13):1509-1519, DOI:10.1080/17568919.2025.2527604.

15. Abulkhair HS, Turky A, Ghiaty A, Ahmed HEA, Bayoumi AH (2020) Novel triazolophthalazine-hydrazone hybrids as potential PCAF inhibitors: design, synthesis, in vitro anticancer evaluation, apoptosis, and molecular docking studies. Bioorganic Chemistry, 100:103899, DOI:10.1016/j.bioorg.2020.103899.

16. Dilek Ö (2025) Comprehensive study of imidazole-based hydrazones: from design, synthesis, and characterization to in vitro and in silico antiproliferative activity analysis. Turkish Journal of Chemistry, 49(4):419-438, DOI:10.55730/1300-0527.3741.

17. Özil M, Önelge E, Emirik M, Acikalin Coskun K, Tutar Y (2026) Trifluoromethyl-benzimidazole-hydrazone derivatives as promising selective anticancer agents: synthesis, cytotoxicity, and molecular docking insights. Pharmaceuticals, 19(8):1270, DOI:10.3390/ph19081270.

18. Kumar R, Chauhan D, Singh VK, Kushwaha AK, Kushwaha D (2025) Design, synthesis, and in-silico studies of hydrazide-hydrazone linked coumarin glycoconjugates with possible antiproliferative activity. Carbohydrate Research, 556:109620, DOI:10.1016/j.carres.2025.109620.

19. Biliz Y, Hasdemir B, Başpınar Küçük H, Zaim M, Şentürk AM, Müdüroğlu Kırmızıbekmez A, Kara İ (2023) Novel N-acyl hydrazone compounds as promising anticancer agents: synthesis and molecular docking studies. ACS Omega, 8(22):20073-20084, DOI:10.1021/acsomega.3c02361.

20. Mosmann T (1983) Rapid colorimetric assay for cellular growth and survival: application to proliferation and cytotoxicity assays. Journal of Immunological Methods, 65(1-2):55-63, DOI:10.1016/0022-1759(83)90303-4.

21. Riccardi C, Nicoletti I (2006) Analysis of apoptosis by propidium iodide staining and flow cytometry. Nature Protocols, 1(3):1458-1461, DOI:10.1038/nprot.2006.238.